Title: Understanding Roman Gold Coinage Inside Out

Authors:

George Alexander Green[1a]*, Katsu Ishida[b], Bethany V. Hampshire[c], Kevin Butcher[a], A. Mark Pollard[d], Adrian D. Hillier[e]

Affiliations:

[a] Department of Classics and Ancient History, University of Warwick; Coventry CV4 7AL, UK.
*Corresponding author. Email: george.green@ashmus.ox.ac.uk
[b] RIKEN Nishina Center, RIKEN; Wako, Saitama 351-0198, Japan.
[c] Department of Physics, University of Warwick; Coventry CV4 7AL, UK.
[d] School of Archaeology, University of Oxford; 1 S Parks Rd, Oxford OX1 3TG, UK.
[e] ISIS Neutron and Muon Facility, STFC Rutherford Appleton Laboratory; Didcot OX11 0QX, UK.

Abstract:

The true purity of Roman silver coinage was hidden by enriching the surfaces of the coins. The question investigated here is whether Roman gold coins were also surfaced enriched. Two non-destructive techniques were employed to do this: X-ray fluorescence (XRF) and a 'newer' technique, muonic X-ray emission spectroscopy (μXES). For the latter, the momentum of the muons is controlled, allowing for the composition of the coin to be determined at various depths. Here we show that there is no surface enrichment of the Roman gold coins analysed. Furthermore, we show that XRF and μXES return congruent results at the near surface. This all supports the integrity of surface level analyses of Roman gold coins. We then discuss the broader applicability of our muon technique to the further study of Roman gold coinage, to the cultural heritage sector and to archaeological scientists more generally.

Key Words:

Roman; Gold; XRF; Muons; non-destructive; μXES; purity.

Abbreviations:

FWHM - Full width at half maximum
RIC - Roman Imperial Coinage Series, Spink Books
μXES - Muonic X-ray emission spectroscopy

[1] Present address: Ashmolean Museum, University of Oxford; Beaumont Street, Oxford OX1 2PH, UK

Introduction:

The use of X-ray fluorescence (XRF) on museum objects has been an established procedure for decades,[1] and has been used on artefacts including Roman statues,[2] Anglo-Saxon gold coins[3] and Japanese ceramics[4] amongst a plethora of other projects.[5] Some museum conservation departments will have their own XRF units, and the non-destructive nature of the technique makes it easy to approve for use on cultural heritage objects. As such, it is a technique that is particularly well known to museum curators. For this reason, it provides a useful reference point to compare more complex or less well known techniques to; especially when seeking to apply these in the cultural heritage sector.

In this case, the 'less well known' technique is the application of negative muons – namely: muonic X-ray emission spectroscopy (μXES).[6] The scientific principles behind this technique are not so far removed from those of XRF. The element that captures the muon emits a characteristic 'fingerprint' of muonic X-rays[7] and a negative muon can, in this case, be considered as an heavy electron. A comparison of the two techniques, then, is quite appropriate. Like XRF, μXES is able to non-destructively analyse the surface of an object and detect elements down to a fraction of 1%. However, by increasing the momentum of the muons we are able to ensure that they penetrate much more deeply into the object.[8,9] An example of this with Roman silver coinage can be seen in Hampshire, *et al.*[6] The exact penetration depth depends on the material, but, generally speaking, this means that we are able to non-destructively analyse both the 'surface' and the 'core' of an object. Analyses that are both non-destructive and penetrative are extremely useful in the study of high value objects that simply cannot be destructively sampled – in this case Roman gold coins.

There are three key questions at hand here. First, can the μXES technique return results for major element composition that are comparable with existing techniques, such as XRF? Second, can the μXES technique when running at a higher momentum penetrate the fabric of gold coins and return useful results from the 'core' of the coin? Finally, can we compare these 'surface' and 'core' measurements in order to determine whether Roman gold coins show any evidence of deliberate surface enrichment?

Below we present results from three Roman gold coins. All of these coins are of significant monetary, historical and artistic value. These were produced by the Emperors Tiberius (Lugdunum mint, AD 14-37, Roman Imperial Coinage volume I, 2nd edition, 29), Hadrian (Rome mint, AD 134-138, RIC III, 280a.) and Julian II 'the Apostate' (Antioch mint, AD 361-363 RIC VIII, 195), and are between approximately 2,000 and 1,600 years old.

Materials and Methods:

X-Ray Fluorescence

The XRF analyses were performed using an Oxford Instruments 'X-MET8000' handheld energy dispersive X-ray fluorescence unit with a voltage of 40 kV, a current of 8 μA and a 1000 μm aluminium filter. The unit contains a rhodium target X-ray tube and a 25mm^2 high resolution silicon-drift detector. This particular analyser comes factory-loaded with fundamental parameters (FP) that are specific to various applications. All analyses here were performed using the pre-loaded 'Precious Metals FP' calibration setting. External standards of known quantities of gold, silver and copper were also used throughout the analysis. On each coin, three separate 10.7mm x 9.4mm spots were

analysed – two on one face of the coin, and one spot on the other. The flattest parts of the coins were chosen for analysis, as irregularly shaped surfaces can affect the accuracy of the results produced.[3,10] The handheld unit was docked into a benchtop stand, and the in-built camera was used to select the spots. Each spot was analysed for 30 seconds – Simsek Franci[11] followed a similar protocol with an X-MET8000 for ceramics - totalling 90 seconds per coin. Quantitative results were extracted using the standard software provided with the unit. These results were then manually compared with the spectra to check for anomalies – sum peaks, escape peaks, diffraction errors and surface contamination[12] – that the standard software did not identify or account for.

In short, the technique itself works by firing an X-ray beam at the sample. This displaces electrons from the inner orbital shells of the atoms in the sampled area, as the energy of the X-ray is greater than the binding energy that holds the electrons in their correct orbits. This creates an electron vacancy leaving the particle in an excited state. Relaxation of the excited state occurs through a cascade of outer electrons falling into lower orbitals. As this occurs X-rays are emitted with energies corresponding to the energy difference between electron orbitals. This energy of this X-ray is characteristic of the element it is emitted from; as such it can be used to quantify the concentrations of the elements present in the sample. The brevity of this explanation is deliberate as dissections of XRF have been undertaken on a number of occasions.[13-16] However, one aspect of the technique worth drawing attention to is that it only returns data from the first few micrometres of the object analysed[3,14,16] – if the surface of the object is not representative of the bulk composition, then it is possible that surface-level XRF results may well be erroneously applied to the object as a whole.

During the XRF analyses three certified alloy standards were used. These were made by Micro-Analysis Consultants Ltd and are referred to as MAC 1, 2 and 3. Each standard was analysed a minimum of six times across the duration of the analyses. The XRF unit was most accurate when analysing MAC 1 (94% Au, 4.5% Ag, 1% Cu) and MAC 2 (75% Au, 19% Ag, 5% Cu) – the results were within a fraction of 1wt% for gold, silver and copper for both of these standards. The margin of error was greater for MAC 3 (59% Au, 30% Ag, 9% Cu), however. This is not particularly a problem here as none of the surfaces of the coins analysed are less than 95% gold, and as such MAC 1 is the much more representative standard. The XRF results for MAC 1 are both accurate and consistent. The largest absolute error for gold was 0.2 percentage points, and the mean absolute error was 0.15 percentage points across the 6 analyses. For silver, the largest absolute error was 0.09 percentage points and the mean absolute error was 0.06 percentage points across the 6 analyses. Outside of this particular experiment, MAC 1 has been analysed 72 times by this handheld unit, and across these 72 analyses the mean absolute error was 0.2 percentage points for gold and 0.06 percentage points for silver. Given all this, the margin of error for the XRF results from the gold coins analysed here is probably significantly less than one percentage point. The mean 2-sigma precision of the gold measurements was ±0.11 and for silver was ±0.02. The full results of all the XRF analyses of the MAC standards can be found in the supplementary material.

Muonic X-ray Emission Spectroscopy

The muon experiments were conducted at the RIKEN-RAL muon beamlines at the ISIS Pulsed Neutron and Muon Facility, STFC Rutherford Appleton Laboratory, UK.[17-19] The negative muons are extracted from a carbon target that is bombarded with high energy protons. This creates pions which are extracted and decay into muons. These muons are momentum selected, which can be from 15 MeV/c up to, currently, 90 MeV/c with a momentum spread of 10% full width at half

maximum (FWHM). This enables a layered compositional analysis of any material to be determined by simply controlling the momentum of the muons, i.e. sampling a thin layer within the material of interest. For pure gold the implantation depth can be controlled between 10s of nanometres to 10s of millimetres. For our experiment, 18 MeV/c and 40 MeV/c were used. The penetration depth of the 18 MeV/c muons was approximately 0.01 mm into the gold coins and for 40 MeV/c approximately 0.4 mm (Figure 1a). The stopping profiles were calculated using SRIM/TRIM (Figure 2).[20] This meant that our 40 MeV/c 'core' analyses penetrated approximately 33% of the way through the c. 1.2 mm thick coin of Tiberius; 40% of the way through the c. 1 mm thick coin of Hadrian; and 50% of the way through the c. 0.8 mm thick coin of Julian II. As such, controlling the momentum of the muons enables the sampling of the 'surface' and 'core' of the coin. The diameter of the muon beam can be varied from ~30 mm to 8 mm. For our experiment the beam was centred on the portraits on the faces of the coins and illuminated the complete cross-section.

Once the negative muons are implanted, at a known depth, they are captured by the constituent atomic elements and form a 'muonic' atom. These negative muons are initially captured, by energy transfer to the Auger electrons, in a high energy electronic state (n≈14) and then cascade down to the lowest state (n=1). This happens in approximately 10^{-13} seconds. Each cascade results in the emission of an X-ray, whose energy is dependent upon the capturing atom (Figure 1b). While a similar process to XRF, the mass of the muon is approximately 207 times that of an electron and results in these muonic X-rays being in the range of 10s keV to MeV (Figure 1c).[21] As such, this results in self-absorption being much less of an issue and enables compositional analysis significantly beneath the surface. Finally, the muon will decay into an electron and a neutrino, or will be captured by the nucleus. If the muon is captured, then a muon and proton reaction can take place and a gamma can be emitted (along with a neutron). The gamma emission can potentially give isotope analysis.[22] All of these emissions are in the order of 10s keV up to approximately 8 MeV and can be detected by high purity germanium detectors.

The experimental setup comprises of four ORTEC high-purity germanium detectors (HPGe), two upstream and two downstream, running the EXP2K software.[23] Each pair of detectors consists of low-energy high-resolution detector (30 keV -1 MeV) and a high-energy lower-resolution detector (50 keV – 8 MeV). The coins were mounted in an aluminium package approximately 0.016mm thick. An image of the experimental setup can be seen in Figure 3, and a fuller description can be found in Hampshire, *et al.*[6] and Hillier, *et al.*[8] For an introductory overview of the technique see Hillier, *et al.*,[24] for a more technical decription see Measday.[21]

Now, concentrating on the details for our experiment. To make the identification of the muonic X-rays easier, elements (purity >99.9%) of the expected significant constituent components were analysed. In this case: gold, silver and copper. The MAC standards used in the XRF measurements were also measured and were used to calibrate the experimental setup, along with a silver/gold mixture (70:30).[25,26] The identification of elements in the gold coins was conducted by using the peak parameters from the pure elements and then varying the silver to gold ratio. These measurements, alongside the statistics collected, show that the minimum composition detectable was approximately 1%. Future detector and instrument improvements should be able to further reduce this. The fits and data can be found in the supplementary information.

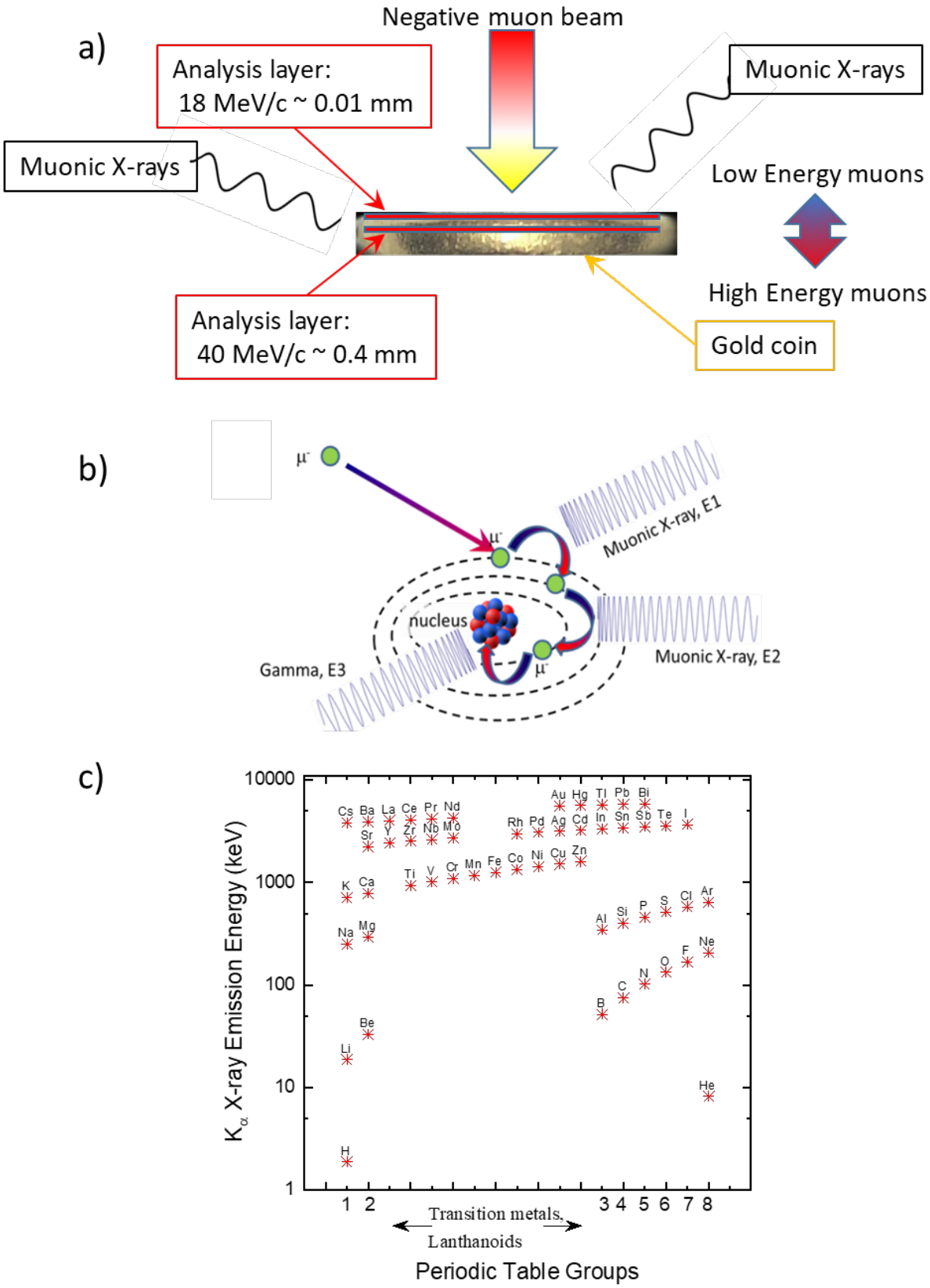

Figure 1 a) A schematic of the implantation process for two muon energies. The higher energy muons are implanted at a deeper depth than the lower energy muons. This is confirmed in Figure 2 which shows the implantation depth profile for the two energies used in this experiment. b) A schematic of the capture process of the muon by an atom to form a

muonic atom. The emissions are also shown from the cascade and capture processes. c) The muonic X-ray emission energy for the K_α transitions. All elements above and including Li can be observed. It is worth noting the y-axis is on a log scale so it is evidently clear that elements next to each other are easily distinguishable.

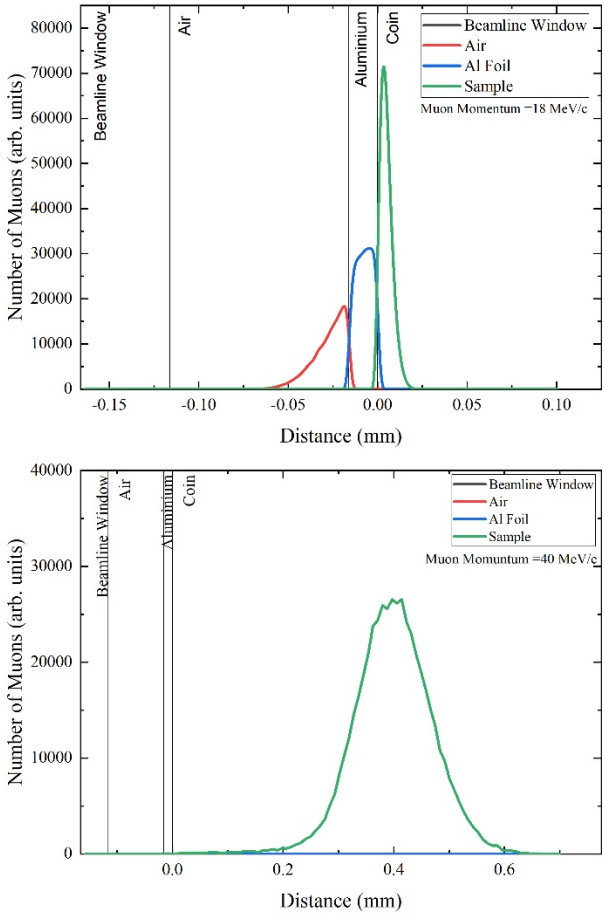

Figure 2 The calculated depth profiles of the negative muons for a given momentum: 18MeV/c (top) and 40MeV/c (bottom). At 18 MeV/c the results clearly comprise of the air, the aluminium packet and the near surface of the gold coin. At 40 MeV/c, the results show the implantation depth is c. 0.4mm. Please note: the air layer is compressed from 100 mm to 0.1 mm to magnify the area of interest (the coin and its holder)

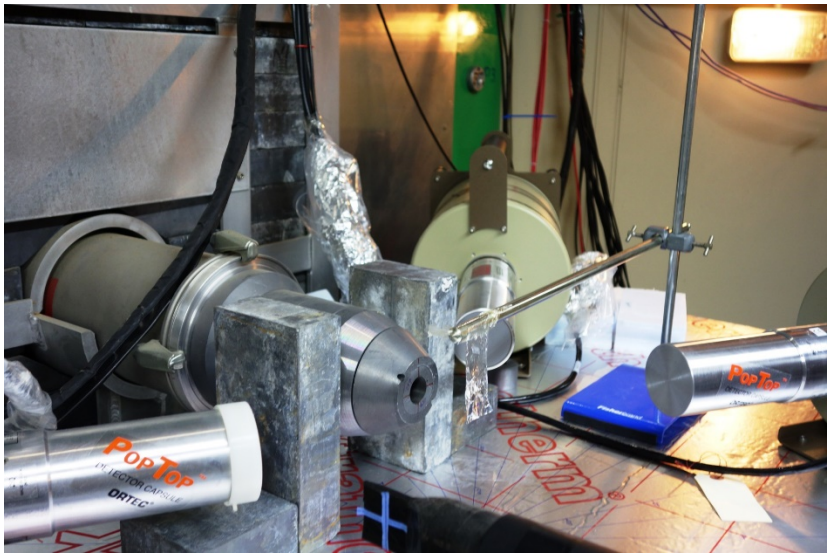

Figure 3 A photo of the experimental setup for measuring the composition of a sample by muonic X-rays. The sample can be found in the aluminium packet held in front of the muon beam. Three of the four HPGe detectors are shown.

Results:

XRF

The XRF results themselves are unsurprising (Table 1). The coins of Tiberius and Hadrian are almost full purity, at 99.7% and 99.6% pure respectively. This is in good agreement with Caley's[27] specific gravity measurements, and their purity will not come as a shock to Roman numismatists. The coin of Julian II is slightly debased, only approximately 95.6% pure, but this broadly matches the figures from Callu, et al.'s[28] proton activation analysis of gold coins from this period. While they did not have access to any coins of Julian II, they did record the gold contents of 13 coins issued between AD 355 and AD 367. These had a mean purity of 95.16%, with a minimum of 93.03% and a maximum of 97.13%. The purity of the coin of Julian II appears to be typical for this particular point in Roman history. The issue with XRF is that these results are only surface level – the first few microns of the coin - and we know that the surface of archaeological gold can differ from the core: the leaching of base metals, for example, is an established phenomenon.[3,14,29,30] Furthermore, we know that Roman silver coins are deliberately surface enriched,[6,31] so it is not unreasonable to be wary of this in the gold.

While techniques that measure the bulk composition can help alleviate some of these issues they come with their own drawbacks. Measuring the bulk composition bundles the measurements from 'surface' and the 'core' together, it does not help us to determine how exactly the two do, or do not, differ. Moreover, specific gravity itself cannot differentiate between silver and copper;[27] and all activation techniques irradiate the sample,[32] which can leave it radioactive and unable to return to the museum for some time. Finally, Oddy[33] has shown that there can be a significant discrepancy between the results of specific gravity, activation analyses and XRF performed using a milliprobe, when analyses were performed on impure gold coins.

We can infer from the available experimental evidence that Roman gold coins were not normally surface enriched. However, these datasets come with methodological caveats or omit coins from the

first and second centuries. As such, what is needed is a technique that can definitively show that the outside of a Roman gold coin is representative of what is on the inside, and that there really is no evidence for deliberate surface enrichment in Roman gold coins across the imperial period. This technique needs to be non-destructive, as Roman gold coins are of high intrinsic, artistic and historical value: routine sectioning, for example, is not an option for museum collections. Equally, it needs to be able to work around the restrictions of cultural heritage institutions: having valuable artefacts out of the museum for long periods of time is not particularly appealing for museum curators, registrars, trustees, or their insurers.

	XRF			µXES - 40 MeV/c			µXES - 18 MeV/c		
Coin [Issue Date]	Mean Au [wt%]	Mean Ag [wt%]	Mean Cu [wt%]	Au [wt%]	Ag [wt%]	Cu [wt%]	Au [wt%]	Ag [wt%]	Cu [wt%]
Tiberius [AD 14-37]	99.73(.01)%	0.27(.01)%	*	>99%	<1%	*	>99%	<1%	*
Hadrian [AD 134-138]	99.55(.01)%	0.45(.01)%	*	>99%	<1%	*	>99%	<1%	*
Julian II [AD 361-363]	95.58(.03)%	4.18(.03)%	0.24(.02)%	96(1)%	4(1)%	*	96(1)%	4(1)%	*

Table 1 A summary of the results obtained from the three Roman gold coins using XRF and µXES. Standard deviation in brackets for XRF, uncertainty in brackets for µXES, asterisk denotes 'below detection'.

The application of negative muons can help us to avoid the methodological drawbacks of XRF and activation analyses. First, µXES is totally non-destructive. Second, it can not only analyse the 'surface' layers of an object, but, by tuning the momentum of the beamline, it can easily penetrate a few hundred microns into the 'core' of the sample. This allows us to characterise these 'layers' separately and take independent measurements for the 'surface' and the 'core' of the object. Finally, the sample is not rendered radioactive after the analysis is complete, meaning it can be handled and, importantly, returned to the museum immediately after the experiment has ended. It is, therefore, an ideal tool for answering questions about the sub-surface composition of high value museum objects.

Interior Composition of the Roman coins

To analyse the 'core' of the coins the momentum of the muon beamline was set to 40 MeV/c (with a momentum spread of 10% full width at half maximum (FWHM), which corresponds to an implantation depth of approximately 0.4 mm. The muonic X-ray emission lines are shown in Figure 4 for the coins we have investigated. The most efficient energy range in terms of data rate and detector performance is between 250–450 keV. As can be seen in Figure 4b-d, all three coins have strong peaks in the 400-410 keV range, which shows that the main element in the gold coins is, unsurprisingly, gold. Looking at the 300-310 keV energy range, where the silver M edges would be expected, no significant peaks can be seen for the coins of Tiberius and Hadrian. It would appear these coins contain less than 1 wt% silver, although this is at the limit of the data quality (±0.9). There are, however, small peaks here for the coin of Julian II. The silver peaks for Julian II correspond to a concentration of approximately 4 wt% (±1.0) silver in a gold matrix. All of these results are in remarkable agreement with the earlier XRF results (Table 1). Therefore, we can conclude that there is no evidence of surface treatment or enrichment in any of the coins that have been investigated.

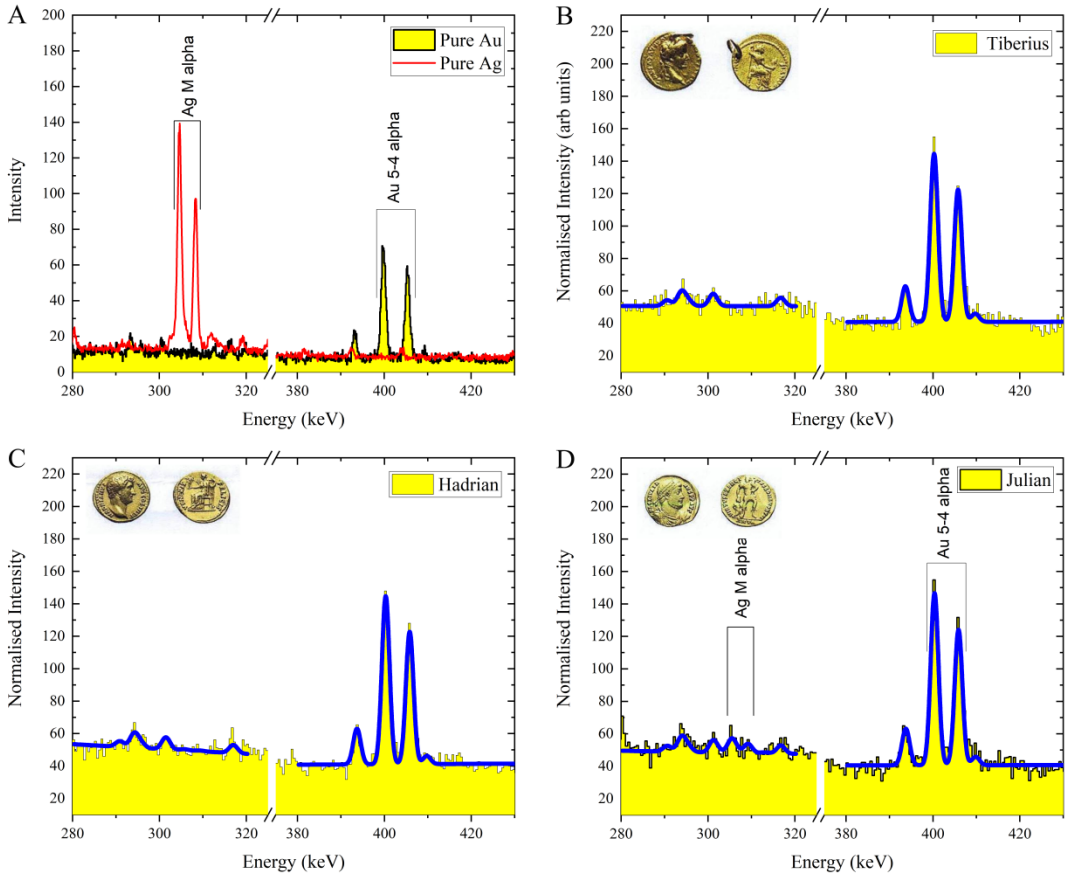

Figure 4 The spectra of the muonic X-rays and gammas over a limited range (290 – 425 keV) from pure gold and silver blanks (A), and the coins of Tiberius (B), Hadrian (C) and Julian II (D). The spectra from the coins have been highlighted in blue. Note the additional silver peaks in the coin of Julian II, highlighted by the vertical bars.

Near-surface/Core comparison

To further support the results from the previous section, the muon momentum was adjusted to 18 MeV/c (again with a momentum spread of 10% FWHM). This enables the composition to be determined close to the surface. As can be seen from Figure 5, we have similar spectra from the 'core' and from the near-surface. At lower muonic X-ray energies, additional peaks from oxygen and nitrogen can be seen (Figure 5a). At 346 keV an additional peak is observed from aluminium (see Figure 5b-d). These extra peaks are from the muons that were stopped by the air gap or the aluminium sample holder respectively. There are no relevant differences between the spectra for the 'surface' and the 'core' of the coins analysed, which again clearly shows that the surface is representative of the bulk composition.

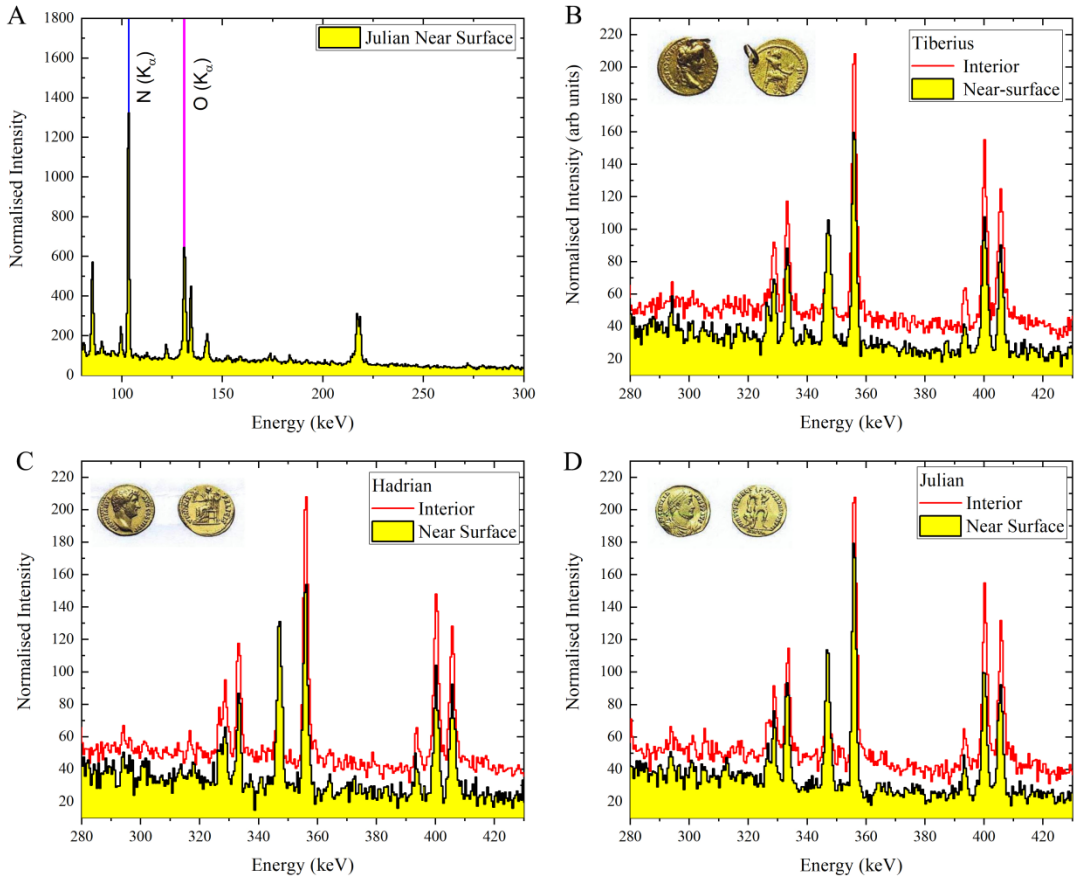

Figure 5 The muonic X-rays and gammas from the interior and near surface of the gold coins of Tiberius (B), Hadrian (C) and Julian II (D).

Discussion:

XRF and µXES returned congruent results for the near-surfaces of the three gold coins analysed (Table 1). The lower and higher momentum µXES analyses returned congruent results for all the coins analysed (Figure 4 and Figure 5). In Roman silver coinage, large differences between the surface and sub-surface can normally be detected well within the first 100 microns.[6,34] The higher momentum µXES analyses penetrated an average of approximately 400 microns (0.4mm) through the faces of the gold coins, which were 0.8-1.2mm thick. It is, therefore, highly improbable that an enriched layer exists.

These µXES results have definitively shown that there is no appreciable difference in the major element composition of the near-surface and the 'core' of the Roman gold coins analysed. The results of this experiment combined with existing specific gravity and activation analyses of Roman gold coinage, provide compelling evidence that Roman gold coins were not normally surface enriched. As such, the hypothesis that this was routinely the case is evidently not correct.

This suggests that the surfaces of Roman gold coins are most probably representative of their bulk composition. This is particularly useful knowledge for researchers involved in the trace element profiling of Roman gold coinage, as this often makes use of surface or near-surface techniques like

laser ablation ICP-MS. Furthermore, this also demonstrates that μXES can be used to determine whether the surfaces of other high value artefacts are representative of their bulk composition, which could then allow surface level trace element techniques to be much more confidently applied to these objects.

At a basic level, it would appear that the high purity gold coins issued by the Roman state in the first and second centuries AD really were very high purity. The early-first century coin of Tiberius and the mid-second century coin of Hadrian clearly show this. This is further evidence of the economic health of the Roman Empire during the middle imperial period. In addition, having confidence that Roman gold coins really were essentially full purity in this period has interesting implications for the discussion of monetary trust in the Roman economy. The weight of the *aureus* was reduced multiple times across the first century BC and AD,[34-37] yet this was seemingly not accompanied by alterations to the purity: this is a deliberate decision and the rationale behind this is historically interesting. On this theme, XRF showed the *solidus* of Julian II to be only approximately 96% pure and μXES confirmed that it was at this purity all the way through. This is interesting, as despite having the technical ability to do so, the Roman state made no attempt to hide the fact that the coin was debased. At this point in time the gold coinage was circulating by weight[38,39] – gold coins were essentially pieces of state-issued bullion in the fourth century AD. A debasement of the gold at this time undermined trust in the value of the coin itself: in this case the state was issuing a c. 4.5g 'gold' piece that really only had c. 4.28g of gold in it. Being confident that gold coins from this later period were not surface enriched allows the ancient historian to explore the various components of monetary trust at this time and to propose why the state chose not to hide the impurity of the gold coinage.

While none of the coins analysed here contained significant concentrations of copper, analyses of the standards show that the μXES technique is able to discriminate between silver and copper at the percentage level. This is important for the study of Roman gold coinage as one potential debasement technique at Rome's disposal is the addition of copper into the gold alloy. Native gold normally contains under 1% copper[40,41] and so the detection of significant quantities of copper in the gold alloy almost certainly indicates its deliberate addition. If copper is detected then we would need to be sure that it is not an artefact of a surface enrichment process. If this is the case, then determining how the copper concentration changes through the fabric of the coin is of utmost importance for investigating the manufacture of that coin. Even if we are confident that the coin is not surface enriched via another analytical technique, it is important to ensure that leaching of copper from the surface into the burial environment has not caused surface-level techniques to understate the true concentration of copper in the coin as a whole. This all requires a non-destructive, penetrative technique that can analyse 'surface' and 'core' independently - the μXES technique is uniquely positioned to do this. At the time of writing, the earliest published copper debasements of Roman gold coinage appear to have been conducted during the 'crisis of the mid-third century'.[28] This means that if significant concentrations of copper are detected in gold coins produced in the preceding 300 years, then the earliest evidence for the use of this debasement technique by the Roman mint could be pushed back quite substantially. The debasements during the AD 68/9 civil wars are a prime area for further investigation of this topic.

In all, the μXES technique is *totally non-destructive*, *penetrative*, requires *no sample preparation*, *does not present a conservation risk* by dirtying or altering the sample, *does not present a safety risk*

by leaving the sample irradiated and can be practicably applied to a *wide range of object sizes.* In addition to this we have shown the technique can produce precise and accurate results for the major element composition of the gold objects analysed. These qualities present many advantages to those working on cultural heritage objects. To start, the muon beam can be safely aimed at the most aesthetically, historically or archaeologically important parts of an object. As a discrete location for penetrative sampling is not necessary, the scholar is able to have much more freedom when investigating their research questions. As sample preparation is not necessary and the objects are not left irradiated, the burden placed on museum administrators and conservation departments is greatly reduced – this means that it is far more probable that the experiment will be approved and the objects released for analysis. Furthermore, as the μXES technique has controlled penetration depths there is no need for freshly-excavated objects to be cleaned, or for corrosion or rust to be removed, before the experiment takes place. Finally, the ability to non-destructively analyse a wide range of sample sizes means even the largest, most valuable cultural heritage objects can have complicated research questions surrounding their composition investigated.

This all leads to a wide variety of potential applications outside of Roman gold coinage. Freshly-excavated objects from shipwrecks or other maritime sites could be analysed with this technique without the need for time-consuming, and potentially destructive, cleaning – this could allow for the objects beneath the mud, rust and corrosion to be safely characterised. Indeed, the layers of corrosion on archaeological objects could be depth profiled using this technique. The same logic can be applied to layers of precious metal gilding, but equally, the technique could be used to investigate the composition of the object beneath such layers. This would be especially pertinent for investigating the manufacturing process of the base object. Identification of different chemical compositions on different parts of the artefact could indicate different manufacturing techniques for certain parts, or sections of the artefact having been worked on at different points in time, before a final outer layer or covering was applied. Given the range of sample sizes possible, this technique could be employed to analyse the interior composition of large statues, sculptures and castings. On the other end of the scale, smaller objects can be completely illuminated by the muon beam, meaning it is hypothetically possible to create a 'heat map' of the concentration of a particular element within the matrix of the object analysed. Finally, μXES can be used to investigate modern or contemporary forgeries, providing that this can be done by detecting the presence of a 'diagnostic' element hidden beneath the surface – for example, gold objects that have a secret core of tungsten.

The application of μXES within the cultural heritage sector is still an underutilised resource, with many muon facilities around the world developing new instrumentation. This means that achievable methodological improvements should allow for further research questions and avenues of investigation to be explored. For example, the sensitivity of the technique is determined by the counting time, the detector efficiencies and the coverage of various angles around the sample by the detectors. A greater number of more efficient detectors should allow for an increase of two orders of magnitude in the sensitivity of the technique. This would be particularly useful for investigating isotope ratios through the detection of gammas or for the detection of minor elements. Equally, these improvements should allow for major element composition to be determined much more quickly, allowing for a greater number of objects to be analysed per day or for especially high value artefacts to be returned to museums more quickly. Finally, improvements to the statistical approaches taken when interpreting the spectra should allow for more precise compositional figures to be obtained.

Conclusions:

XRF and µXES returned congruent results for the near-surfaces of the three Roman gold coins analysed, showing that the two techniques can produce comparable results. The advantage of µXES over XRF is that the negative muons can be given a higher momentum in order to penetrate approximately 400 microns into the gold coin. In this case we have used this to provide additional, compelling evidence that Roman gold coins were not routinely surface enriched. This is a useful conclusion for research groups using near-surface trace element techniques on Roman gold coins, as it shows the 'surface' is representative of the 'core' of the coin. The lack of surface enrichment in the debased coin of Julian II is particularly interesting. Furthermore, having confidence that Roman gold coinage is not surface enriched allows for the nature of monetary trust in the Roman economy to be explored in more depth.

These results also show the potential of the µXES technique to be applied more broadly in the cultural heritage sector. The technique is totally non-destructive, penetrative, clean and safe. It requires no sample preparation and can be applied to a wide range of object sizes. It is, therefore, an ideal tool for answering questions about the sub-surface composition of high value museum objects. Potential broader applications include, but are not limited to: depth profiling the corrosion on an artefact; determining the interior composition of statues; profiling a gilded layer on an object; the determination of 'hidden' signatures of both modern and contemporary forgeries; and identifying chemical changes during the manufacturing process.

References:

1 Hall, E. T., Schweizer, F. & Toller, P. A. X-Ray Fluorescence Analysis of Museum Objects: A New Instrument *Archaeometry* **15**, 53-78 (1973).

2 Kopczynski, N. *et al.* Polychromy in Africa Proconsularis: Investigating Roman Statues using X-ray Fluorescence Spectroscopy. *Antiquity* **91**, 139-154 (2017).

3 Blakelock, E. S. Never Judge A Gold Object by Its Surface Analysis: A Study of Surface Phenomena in a Selection of Gold Objects From the Staffordshire Hoard. *Archaeometry* **58**, 912-929 (2016).

4 Hall, M. Pottery production during the Late Jomon period: insights from the chemical analyses of Kasori B pottery. *Journal of archaeological science* **31**, 1439-1450 (2004).

5 Liss, B. & Stout, S. in *Heritage and Archaeology in the Digital Age: Acquisition, Curation, and Dissemination of Spatial Cultural Heritage Data* (eds Matthew L. Vincent, Víctor Manuel López-Menchero Bendicho, Marinos Ioannides, & Thomas E. Levy) 49-65 (Springer International Publishing, 2017).

6 Hampshire, B. *et al.* Using Negative Muons as a Probe for Depth Profiling Silver Roman Coinage. *Heritage* **2**, 400-407 (2019).

7 Zinatulina, D. *et al.* Electronic catalogue of muonic X-rays. *EPJ Web Conf.* **177**, 03006 (2018).

8 Hillier, A. D., Paul, D. & Ishida, K. Probing beneath the surface without a scratch — Bulk non-destructive elemental analysis using negative muons. *Microchemical journal* **125**, 203-207, doi:10.1016/j.microc.2015.11.031 (2016).

9 Clemenza, M. *et al.* Muonic atom X-ray spectroscopy for non-destructive analysis of archeological samples. *Journal of Radioanalytical and Nuclear Chemistry* **322**, 1357-1363, doi:10.1007/s10967-019-06927-6 (2019).

10 Geil, E. C. & Thorne, R. E. Correcting for surface topography in X-ray fluorescence imaging. *Journal of synchrotron radiation* **21**, 1358-1363 (2014).

11 Simsek Franci, G. Handheld X-ray Fluorescence (XRF) Versus Wavelength Dispersive XRF: Characterization of Chinese Blue-and-White Porcelain Sherds Using Handheld and Laboratory-Type XRF Instruments. *Applied Spectroscopy* **74**, 314-322 (2020).
12 Tanaka, R., Yuge, K., Kawai, J. & Alawadhi, H. Artificial peaks in energy dispersive X-ray spectra: sum peaks, escape peaks, and diffraction peaks: Artificial peaks in energy dispersive X-ray spectra. *X-Ray Spectrometry* **46**, 5-11 (2017).
13 Karydas, A. G. Application of a Portable XRF Spectrometer for the Non-invasive Analysis of Museum Metal Artefacts. *Annali di Chimica* **97**, 419-432 (2007).
14 Hall, E. T. Surface enrichment of buried metals. *Archaeometry* **4**, 61-66 (1961).
15 Cowell, M. R. in *Metallurgy in Numismatics* Vol. 4 (eds W. A. Oddy & M. R. Cowell) 448-460 (Royal Numismatic Society, 1998).
16 Van Grieken, R. & Markowicz, A. *Handbook of X-Ray Spectrometry*. 2nd edn, (Marcel Dekker, Inc., 2001).
17 Matsuzaki, T. *et al.* The RIKEN-RAL pulsed Muon Facility. *Nuclear Instruments and Methods in Physics Research Section A: Accelerators, Spectrometers, Detectors and Associated Equipment* **465**, 365-383, doi:https://doi.org/10.1016/S0168-9002(01)00694-5 (2001).
18 Hillier, A. D., Lord, J. S., Ishida, K. & Rogers, C. Muons at ISIS. *Philosophical Transactions of the Royal Society A: Mathematical, Physical and Engineering Sciences* **377**, 20180064, doi:10.1098/rsta.2018.0064 (2019).
19 Thomason, J. W. G. The ISIS Spallation Neutron and Muon Source—The first thirty-three years. *Nuclear Instruments and Methods in Physics Research Section A: Accelerators, Spectrometers, Detectors and Associated Equipment* **917**, 61-67, doi:https://doi.org/10.1016/j.nima.2018.11.129 (2019).
20 Ziegler, J. F., Ziegler, M. D. & Biersack, J. P. SRIM – The stopping and range of ions in matter. *Nuclear instruments & methods in physics research. Section B, Beam interactions with materials and atoms* **268**, 1818-1823 (2010).
21 Measday, D. F. The nuclear physics of muon capture. *Physics Reports* **354**, 243-409, doi:10.1016/S0370-1573(01)00012-6 (2001).
22 Ninomiya, K. *et al.* in *Proceedings of the 14th International Conference on Muon Spin Rotation, Relaxation and Resonance (?SR2017)* Vol. 21 *JPS Conference Proceedings* (Journal of the Physical Society of Japan, 2018).
23 Nakamura, S. N. & Iwasaki, M. A new data acquisition system for the RIKEN-RAL μCF experiment. *Nuclear Instruments and Methods in Physics Research Section A: Accelerators, Spectrometers, Detectors and Associated Equipment* **388**, 220-225, doi:https://doi.org/10.1016/S0168-9002(97)00343-4 (1997).
24 Hillier, A., Hampshire, B. & Ishida, K. in *Handbook of Cultural Heritage Analysis* (eds Sebastiano D'Amico & Valentina Venuti) (Springer Nature Switzerland AG 2021).
25 Hillier, A. D. *et al.* How low can you go? *STFC ISIS Neutron and Muon Source*, doi:10.5286/ISIS.E.RB1820616-1 (2019).
26 Hillier, A. D. *et al.* Using negative muons as a non-destructive probe of material composition. *STFC ISIS Neutron and Muon Source*, doi:10.5286/ISIS.E.RB1510343 (2015).
27 Caley, E. R. Estimation of Composition of Ancient Metal Objects. *Analytical Chemistry* **24**, 676-681 (1952).
28 Callu, J. P., Brenot, C., Barrandon, J. N. & Poirier, J. in *L'Or monnayé I. Purification et altérations de Rome à Byzance (Cahiers Ernest-Babelon II)* (eds C Morrisson *et al.*) 81-111 (Centre National de la Recherche Scientifique, 1985).
29 Hook, D. R. & Needham, S. P. A comparison of recent analyses of British Late Bronze Age goldwork with Irish parallels. *Jewellery Studies* **3**, 15-24 (1989).
30 Tate, J. Some problems in analysing museum material by nondestructive surface sensitive techniques. *Nuclear Instruments and Methods in Physics Research* **14**, 20-23 (1986).

31 Butcher, K. & Ponting, M. The Roman Denarius Under the Julio-Claudian Emperors: Mints, Metallurgy and Technology. *Oxford Journal of Archaeology* **24**, 163-197 (2005).
32 Segeblade, C. & Berger, A. in *Encyclopedia of Analytical Chemistry: Applications, Theory and Instrumentation* (ed R A Meyers) (John Wiley, 2008).
33 Oddy, W. A. The Analysis of Gold Coins — A Comparison of Results Obtained by Non-Destructive Methods. *Archaeometry* **14**, 109-117 (1972).
34 Butcher, K., Ponting, M., Evans, J., Pashley, V. & Somerfield, C. *The Metallurgy of Roman Silver Coinage: From the Reform of Nero to the Reform of Trajan*. (Cambridge University Press, 2014).
35 Woytek, B. in *The Oxford Handbook of Greek and Roman Coinage* (ed W E Metcalf) 315-331 (Oxford University Press, 2012).
36 Duncan-Jones, R. *Money and Government in the Roman Empire*. (Cambridge University Press, 1994).
37 Green, G. A. *Gold Coinage in the Roman World: Function and Production* Doctor of Philosophy thesis, University of Warwick, (2021).
38 Erim, K. T., Reynolds, J. & Crawford, M. Diocletian's Currency Reform; A New Inscription. *The Journal of Roman Studies* **61**, 171-177 (1971).
39 Abdy, R. in *The Oxford Handbook of Greek and Roman Coinage* (ed W E Metcalf) 584-600 (Oxford University Press, 2012).
40 Guerra, M. F. & Calligaro, T. Gold traces to trace gold. *Journal of Archaeological Science* **31**, 1199–1208 (2004).
41 Raub, C. J. in *Prehistoric Gold in Europe,* (eds G Morteani & J P Northover) 243-260 (Kluwer Academic Publishers, 1995).

Acknowledgements:

Funding

Arts and Humanities Research Council, Collaborative Doctoral Partnership Studentship (GAG)
Leverhulme Trust, Early Career Fellowship (GAG)
ISIS Neutron and Muon Facility, STFC Rutherford Appleton Laboratory, 'In-kind' contribution of muon beam time (GAG, KI, BVH, KB, AMP, ADH)

Any funders had no input into this piece of work.

Author Contributions

Conceptualization: GAG, KI, BVH, KB, AMP, ADH

Methodology: GAG, KI, BVH, ADH

Investigation: GAG, KI, BVH, KB, AMP, ADH

Visualization: GAG, KI, ADH

Funding acquisition: GAG, KI, KB, AMP, ADH

Project administration: GAG, KI, ADH

Writing – original draft: GAG, ADH

Writing – review & editing: KI, BVH, KB, AMP

Competing interests

Authors declare that they have no competing interests.

Data Availability

All data are available in the main text and the supplementary materials.